FUSION OF OUT OF FOCUS IMAGES USING PRINCIPAL COMPONENT ANALYSIS AND SPATIAL FREQUENCY

V.P.S. Naidu* and J.R. Raol*

Abstract

Details of principal component analysis and spatial frequency are presented. Two image fusion architectures are developed to fuse multi focused images and their performance is compared. In first architecture source images to be fused are considered as whole in the fusion process. In second architecture the source images to be fused are divided into blocks and then used in the fusion process. Overall SF shows slightly better performance. Block based image fusion scheme (second architecture) shows superior performance. This architecture is very simple and can be used in real time applications.

***Keywords**: PCA, Spatial Frequency, Image Fusion, Fusion Performance Index*

Nomenclature

λ	= eigenvalue
CF	= column frequency
h_{I_f}	= normalized histogram
I_1 and I_2	= source images to be fused
I_f	= fused image
I_r	= reference or ground truth image
I_{1k} and I_{2k}	= k^{th} block source images
L	= number of gray levels
NSF_i	= i^{th} principal component
NPC_i	= i^{th} principal component
RF	= row frequency
SF	= spatial frequency
th	= threshold
V	= orthogonal projection matrix
X	= random vector
DCT	= Discrete Cosine Transform
FFT	= Fast Fourier Transform
MSIF	= Multi Sensor Image Fusion
PCA	= Principal Component Analysis
PFE	= Percentage Fit Error
PSNR	= Peak Signal to Noise Ratio
RMSE	= Root Mean Square Error
SD	= Standard Deviation
SF	= Spatial Frequency

Introduction

Single imaging sensor cannot provide complete information about a situation. Multi imaging sensor fusion would provide better or enhanced information about the situation. Off late multi sensor fusion has emerged as an innovative and promising research area. Sensor fusion could take place at signal level, pixel level, feature level and symbol level [1]. Multi sensor image fusion (MSIF) is a technique for merging the registered multi sensor images to enhance the image information. The fused image has improved contrast and it could be easy for the user to detect, recognize and identify the targets and increase users situational awareness [2]. The fusion of images is of vast significance in numerous applications viz. microscopic imaging, medical imaging, remote sensing, robotics and computer vision. Some common requirements would be imposed on the fusion results: (1) fused image should preserve all relevant information contained in the source images, (2) fusion process would not introduce any artifacts or inconsistencies which would amuse the human observer or following processing stages and (3) irrelevant features and noise should be suppressed in the fused image to a maximum extent [3]. When image fusion is done at pixel level the source images are combined without any pre-processing. The pixel level fusion (also called image level fusion) algorithms vary from simple image averaging to very complex algorithms. The simplest MSIF is to take the average of the grey level source images pixel by pixel. This technique would produce several undesired

* Scientist, Multi Sensor Data Fusion Laboratory, Flight Mechanics and Control Division, National Aerospace Laboratories, Post Box No. 1779, Bangalore-560 017, India, Email : vpsnaidu@gmail.com
Manuscript received on 06 Nov 2007; Paper reviewed, revised and accepted on 13 May 2008

effects and reduced feature contrast. To overcome this problem, multi-scale transforms, such as wavelets, Laplacian pyramids, morphological pyramid and gradient pyramid have been proposed. Multi-resolution wavelet transforms could provide good localization in both spatial and frequency domains. Discrete wavelet transform would provide directional information in decomposition levels and contain unique information at different resolutions [4, 5].

In some situations the objects in the scene would be at different distances from the imaging sensor. Inexpensive sensor would not focus everywhere. If one object is in focus then another will be out of focus. Fusing these images there would be little out of focus in the fused image [6]. In this paper, an efficient image level fusion algorithms based on principal component analysis and spatial frequency are proposed. Two different fusion architectures are evaluated. In former architecture source images to be fused are considered as whole in the fusion process. There would be some discrepancy in the fused image that local variations (level of focus) in the source images are not considered. In second architecture the source images are decomposed into small blocks and these blocks are used in the image fusion process. In this the discrepancy would be reduced since the local variations are considered in the fusion process. In Ref. 6, block size and threshold are user defined parameters utilized in the second architecture. It could be very hard to choose the threshold to get optimal fusion results. In this paper, a modified algorithm that computes normalized spatial frequencies is introduced in the fusion process. Since the spatial frequencies of source images are normalized, the user can choose the threshold in between 0 to 0.5. Similar methodology is adopted for principal component analysis based image fusion algorithm. Since choosing of block size and threshold is complex, a simple solution is provided to get the optimal fusion results at the cost of execution time. The performances of these algorithms are evaluated with performance evaluation metrics.

One of the important prerequisites to be able to apply fusion techniques to source images is the image registration i.e., the information in the source images needed to be adequately aligned and registered prior to fusion of the images. In this paper, it is assumed that the source images are already registered.

Fusion Algorithms

The details of principal component analysis and spatial frequency computations are described in this section.

Principal Component Analysis

Principal component analysis (PCA) involves a mathematical procedure that transforms a number of correlated variables into a number of uncorrelated variables called principal components. PCA computes a compact and optimal description of the data set. The first principal component accounts for as much of the variance in the data as possible and each succeeding component accounts for as much of the remaining variance as possible. First principal component is taken to be along the direction with the maximum variance. The second principal component is constrained to lie in the subspace perpendicular of the first. Within this subspace, this component points the direction of maximum variance. The third principal component is taken in the maximum variance direction in the subspace perpendicular to the first two and so on. PCA is also called as Karhnen- Loeve transform or the Hotelling transform. PCA does not have a fixed set of basis vectors like FFT, DCT and wavelet etc. and its basis vectors depend on the data set. PCA is used extensively in image compression and image classification.

Let X be a d-dimensional random vector and assume it to have zero empirical mean. Orthonormal projection matrix V would be such that $Y = V^T X$ with the following constraints. The covariance of Y, i.e. cov(Y) is a diagonal and inverse of V is equivalent to its transpose. Using matrix algebra [7].

$$\begin{aligned} \mathrm{cov}(Y) &= E\{YY^T\} \\ &= E\{(V^T X)(V^T X)^T\} \\ &= E\{(V^T X)(X^T V)\} \\ &= V^T E\{XX^T\} V \\ &= V^T \mathrm{cov}(X) V \end{aligned} \tag{1}$$

Multiplying both sides of (Eq.1) by V, one would get

$$\begin{aligned} V\,\mathrm{cov}(Y) &= V V^T \mathrm{cov}(X) \\ &= \mathrm{cov}(X) V \end{aligned} \tag{2}$$

One could write V as $V = [V_1, V_2, \ldots, V_d]$ and cov (Y) in the diagonal from as :

$$\begin{bmatrix} \lambda_1 & 0 & \dots & 0 & 0 \\ 0 & \lambda_2 & \dots & 0 & 0 \\ \dots & \dots & \dots & \dots & \dots \\ 0 & 0 & \dots & \lambda_{d-1} & 0 \\ 0 & 0 & \dots & 0 & \lambda_d \end{bmatrix} \tag{3}$$

By substituting (Eq.3) into (Eq.2) :

$$\left[\lambda_1 V_1, \lambda_2 V_2, \dots, \lambda_d V_d\right]$$
$$= \left[\operatorname{cov}(X)\, V_1, \operatorname{cov}(X)\, V_2, \dots, \operatorname{cov}(X)\, V_d\right] \tag{4}$$

This could be rewritten as :

$$\lambda_i V_i = \operatorname{cov}(X)\, V_i \tag{5}$$

where $i = 1, 2, ..., d$

V_i is an eigenvector of cov (X)

PCA Algorithm

Let the source images (images to be fused) be arranged in two column vectors. The steps followed to project this data into a two dimensional subspaces are:

- Organize the data into column vectors. The resulting matrix Z is of dimension nx2.
- Compute the empirical mean along each column. The empirical mean vector M has a dimension of 2 x 1.
- Subtract the empirical mean vector M from each column of the data matrix Z. The resulting matrix X is of dimension nx2.
- Find the covariance matrix C of S i.e. $C = X^T X$.
- Compute the eigenvectors V and eigenvalue D of C and sort them by decreasing eigenvalue. Both V and D are of dimension 2 x 2.
- Consider the first column of V which corresponds to larger eigenvalue to compute the principal components NPC_1 and NPC_2 as:

$$NPC_1 = \frac{V(1)}{\sum V} \text{ and } NPC_2 = \frac{V(2)}{\sum V} \tag{6}$$

Image Fusion by PCA

The information flow diagram of PCA based weighted average image fusion algorithm (first architecture) is shown in Fig.1a. The source images (images to be fused) I_1 and I_2 are arranged in two column vectors and their empirical means are subtracted. The resulting vector has a dimension of nx2, where n is length of the each image vector. Eigenvector and eigenvalues for this resulting vector are computed and the eigenvectors corresponding to the larger eigenvalue are obtained. The principal components NPC_1 and NPC_2 (i.e. $NPC_1 + NPC_2 = 1$) using eq.6 are computed from the obtained eigenvector. The fused image is obtained by:

$$I_f = NPC_1 I_1 + NPC_2 I_2 \tag{7}$$

The information flow diagram of PCA based block image fusion algorithm (second architecture) is shown in Fig.1b. The input images are decomposed into blocks (I_{1k} and I_{2k}) of size m x n. Where I_{1k} and I_{2k} denotes the kth blocks of I_1 and I_2 respectively. Principal components for each block using Eq.6 are computed. Let the principal components corresponding k^{th} blocks be NPC_{1k} and NPC_{2k} (i.e. $NPC_{1k} + NPC_{2k}$).The fusion of k^{th} block of the fused image is:

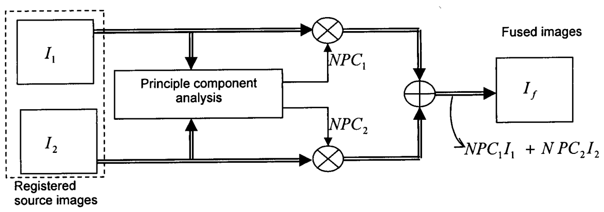

Fig.1a Information flow diagram of PCA based weighted image fusion algorithm

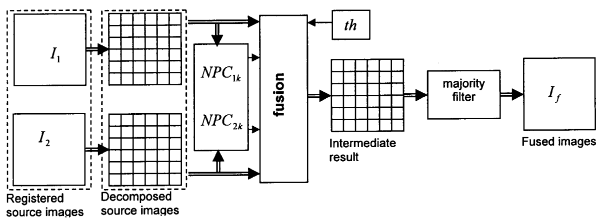

Fig.1b Information flow diagram of PCA based block image fusion algorithm

$$I_{fk} = \begin{cases} I_{1k} & NPC_{1k} > NPC_{2k} + th \\ I_{2k} & NPC_{1k} < NPC_{2k} - th \\ \dfrac{I_{1k} + I_{2k}}{2} & otherwise \end{cases} \tag{8}$$

where th : user defined threshold

$\dfrac{I_{1k} + I_{2k}}{2}$: gray level averaging of corresponding pixels

Spatial Frequency

Spatial frequency measures the overall information level in an image [6,8]. The spatial frequency for a given image I of dimension $M \times N$ is defined as follows:

Row Frequency :

$$RF = \sqrt{\frac{1}{MN} \sum_{i=0}^{M-1} \sum_{j=1}^{N-1} [I(i,j) - I(i,j-1)]^2} \tag{9}$$

Column Frequency :

$$CF = \sqrt{\frac{1}{MN} \sum_{j=0}^{N-1} \sum_{i=1}^{M-1} [I(i,j) - I(i,-1,j)]^2} \tag{10}$$

Spatial Frequency :

$$SF = \sqrt{RF^2 + CF^2} \tag{11}$$

where

M = number of rows; N = number of columns
(i, j) = pixel index ; I = given image
I (i, j) = gray value at pixel (i, j)

Image Fusion by SF

The information flow diagram of SF based weighted image fusion algorithm (first architecture) is shown in Fig.2a. Denote the SF_1 and SF_2 spatial frequencies of input images I_1 and I_2 respectively. The computed spatial frequencies are then normalized as:

$$NSF_1 = \frac{SF_1}{SF_1 + SF_2} \text{ and } NSF_2 = \frac{SF_2}{SF_1 + SF_2} \tag{12}$$

The fused image is obtained by

$$I_f = NSF_1 I_1 + NSF_2 I_2 \tag{13}$$

The information flow diagram of SF based block image fusion algorithm (second architecture) is shown in Fig.2b. The input images are decomposed into blocks (I_{1k} and I_{2k}). Normalized spatial frequencies for each block using Eq.12 are computed. Denote the normalized spatial frequencies of I_{1k} and I_{2k} by NSF_{1k} and NSF_{2k} respectively. The fusion of the k^{th} block of the fused image is:

$$I_{fk} = \begin{cases} I_{1k} & NSF_{1k} > NSF_{2k} + th \\ I_{2k} & NSF_{1k} < NSF_{2k} - th \\ \dfrac{I_{1k} + I_{2k}}{2} & otherwise \end{cases} \tag{14}$$

Majority Filter

In block image fusion algorithm, majority filter is used to avoid the artifacts in fused image caused by the fusion rules. If the center block comes from I_1 and the surroundings blocks are from I_2 then the centre block will be replaced by the block from I_2 and vise versa [7].

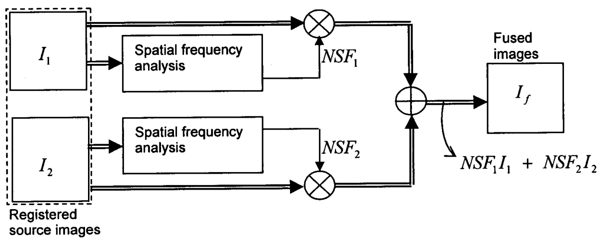

Fig.2a Information flow diagram of SFA based weighted image fusion algorithm

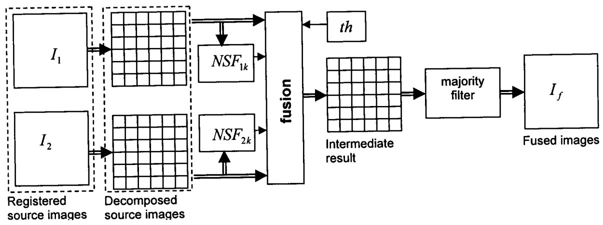

Fig.2b Information flow diagram of SFA based block image fusion algorithm

The majority filter with the order of 3 x 3 is used in this study.

Example: Majority filter working principal is demonstrated here. Denote *a* and *b* as the block images coming from I_1 and I_2 respectively. A block window in the thematic map is shown in left side. One can see that the blocks (a) from I_1 is six times and blocks (b) from I_2 is three times. The majority filter replaces the centre block with the block coming from I_1, since the majority of neighboring blocks are coming from the I_1.

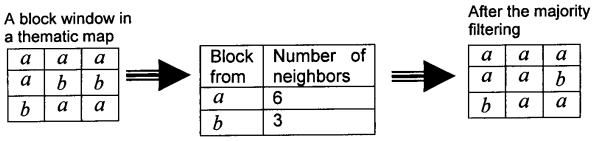

Performance Evaluation

With Reference Image

When the reference image is available, the performance of image fusion algorithms can be evaluated using the following metrics.

- Root Mean Square Error (RMSE) [9]

This metric is computed as the root mean square error of the corresponding pixels in the reference image I_r and the fused image I_f. This metric will be nearly zero when the reference and fused images are similar. This will increase when the dissimilarity increases.

$$RMSE = \sqrt{\frac{1}{MN} \sum_{i=1}^{M} \sum_{j=1}^{N} \left(I_r(i,j) - I_f(i,j-1) \right)^2} \quad (15)$$

- Percentage Fit Error (PFE) [9]

This metric is computed as the norm of the difference between the corresponding pixels of reference and fused image to the norm of the reference image. This will be zero when both reference and fused images are exactly alike and it will be increased when the fused image is deviated from the reference image.

$$PFE = \frac{norm\,(I_r - I_f)}{norm\,(I_r)} * 100 \quad (16)$$

where is the operator to compute the largest singular value.

- Peak Signal to Noise Ratio (PSNR) [10]

Its value will be high when the fused and reference images are similar. Higher value implies better fusion. The peak signal to noise ratio is computed as:

$$PSNR = 20 1og_{10} \left(\frac{L^2}{\frac{1}{MN} \sum_{i=1}^{M} \sum_{j=1}^{N} \left(I_r(i,j) - I_f(i,j-1) \right)^2} \right) \quad (17)$$

where L in the number of gray levels in the mage

Without Reference Image

When the reference image is not available, the performance of image fusion algorithms can be evaluated using the following metrics.

- Standard Deviation [11]

It is known that standard deviation is composed of the signal and noise parts. This metric would be more efficient in the absence of noise. It measures the contrast in the fused image. An image with high contrast would have a high standard deviation.

$$\sigma = \sqrt{\sum_{i=0}^{L} (i - \bar{i})^2 h_{I_f}(i)}, \quad \bar{i} = \sum_{i=0}^{L} i h_{I_f} \quad (18)$$

where

$h_{I_f}(i)$ is the normalized histogram of the fused image $I_f(x, y)$ and L number of frequency bins in the histogram.

- Spatial Frequency [8]

This frequency in spatial domain indicates the overall activity level in the fused image. It is computed using the Eq.11.

The fused image with higher SF has to be chosen, since SF shows the overall information content in the image.

Results and Discussion

The ground truth image I_t is shown in Fig.3a. The source images I_1 and I_2 to be fused are shown in Fig.3b. The source images have been created by blurring the some portions of the reference image with a Gaussian mask using diameter of 12 pixels. The fused & error images by PCA and SF with the procedure given in first architecture are shown in Fig.4a and 4b respectively. Performance evaluation metrics are shown in Table-1. From these results it is observed that image fusion by SF is marginally better.

Figure 5a shows an 100 x 100 image block and Fig.5b to d show the degraded versions after blurring with a disk of radius 5, 9 and 21pixels respectively. Fig.5a is taken as one of the source images I_1 and the blurred image is taken as another source image I_2. The computed principal components and normalized spatial frequencies are shown in Table-2. Fig.6 shows the principal components and normalized spatial frequencies with respect to increase in the amount of blur. It is observed that second principal component and spatial frequency are diminished as the images get more blurred. The rate of change of principal components and normalized spatial frequencies are shown in Fig.7. It is observed that the rate of change of SF is high. Hence, SF would be better indicator of the degradation.

The performance metrics for different thresholds and block sizes are shown in Tables-3 and 4. It is observed that threshold greater than 0.1 incase of PCA and 0.15 incase

Fig.3a Ground truth image (I_t)

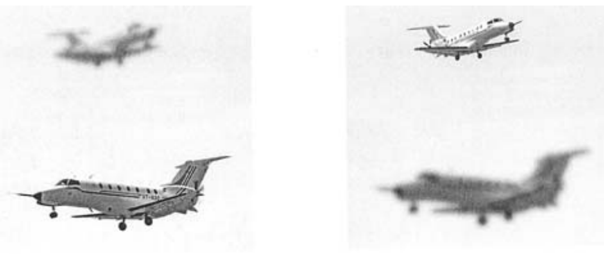

(a) Image I_1 (b) Image I_2

Fig.3b Source images to be fused

Table-1 : Performance evaluation metrics (first architecture)					
	RMSE	PFE	PSNR	SD	SF
PCA	9.3383	4.0057	38.4621	45.9203	9.1679
SF	9.2249	3.9570	38.5152	45.9901	9.2496

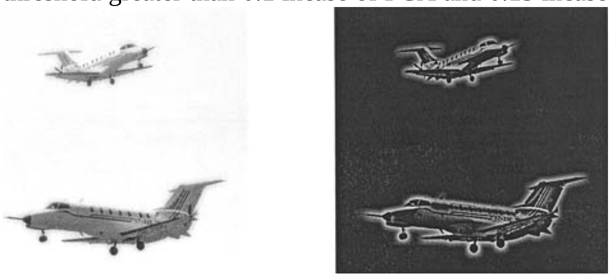

Fig.4a Fused and error images by PCA

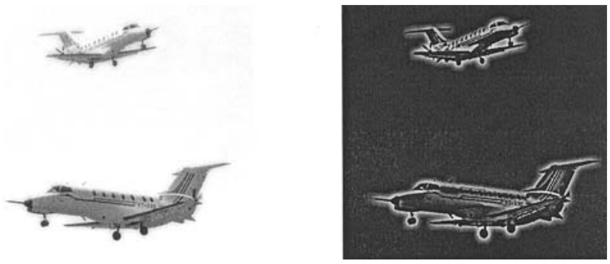

Fig.4b Fused and error images by SF

(a) (b) (c) (d)

Fig.5 Original and its blurred versions with standard deviation of 10 (a) radius = 0 pixels; (b) radius = 5 pixels; (c) radius = 9 pixels; (d) radius = 21pixels

Table-2 : Principal components and normalized spatial frequencies of blurred images				
	Radius=0	Radius=5	Radius=9	Radius=21
NPC1	0.5	0.5347	0.5611	0.6213
NPC2	0.5	0.4653	0.4389	0.3787
NSF1	0.5	0.7197	0.83	0.8936
NSF2	0.5	0.2803	0.17	0.1064

of SF show the degraded performance. The fusion algorithm becomes gray level averaging of corresponding pixels when the chosen threshold is too high (see Eq. 8 and 14). And block sizes 4 x 4, 8 x 8 and 32 x 32 show the degraded performance in both PCA and SF. The fused and error images by PCA and SF are shown in Fig.8a and 8b respectively with block size 64 x 64 and *th* = 0.025. Table-5 shows the performance evaluation metrics. It is observed that SF shows slightly better performance. Fig.9a and Fig.9b show the fused and error images by PCA and SF respectively with block size 4 x 4 and *th* = 0.2. And and Table-6 shows the performance evaluation metrics. It is observed that in this situation also SF showed slightly better performance.

SF shows slightly better performance. Block based image fusion scheme (second architecture) shows enhanced performance. It could be due to the consideration of local variations presented in the source images. Selection of block size and threshold are very difficult in practice. One way to obtain optimal fusion image is, compute the performance of the fusion for different combination of block sizes and thresholds and then select the fused image corresponding to maximum value from the performance metrics.

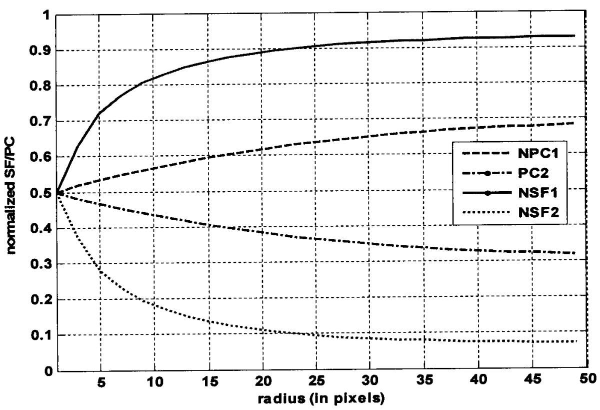

Fig.6 Normalized spatial frequencies and principal components for varying radius and standard deviation of 10

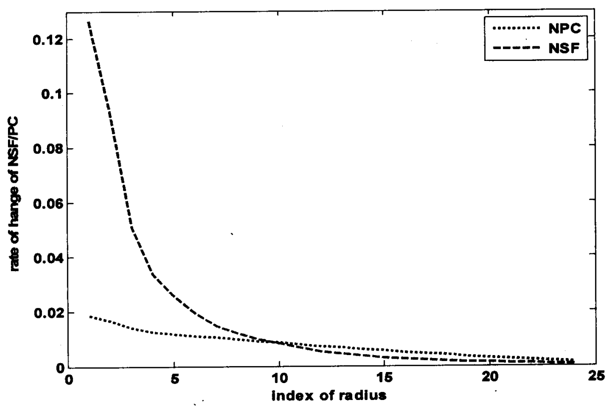

Fig.7 Rate of change of NSF/NPC with magnitude blur

Table-3a : RMSE of fused image by PCA for different thresholds and block sizes

th	4x4	8x8	16x16	32x32	64x64	128x128	256x256
0	8.0595	6.5148	3.8312	0.0880	0.7468	0.8170	0.0214
0.025	8.0261	6.5426	3.8312	0.0882	0.7468	0.8170	0.0214
0.05	8.0046	6.5426	3.8312	0.0882	0.7468	0.8170	0.0214
0.075	7.9869	6.5014	3.8311	0.0702	0.7468	7.7641	7.5779
0.1	7.9500	6.5014	3.8311	0.0702	0.7530	8.8116	7.5779
0.125	7.9454	6.5012	3.8311	0.0702	0.7539	8.8116	7.5779
0.15	7.9717	6.5208	3.8311	0.0702	0.7695	9.2799	7.5779
0.175	7.9111	6.4796	3.8311	0.0848	0.7695	9.2799	9.4173
0.2	7.9420	6.4796	3.8311	0.0932	1.3909	9.9585	9.4173
0.225	8.0528	6.5012	3.8311	0.0932	2.5048	10.5712	9.4173
0.25	8.0637	6.5454	3.8311	0.1074	2.5068	9.9022	9.4173
0.275	8.0652	6.5080	3.8311	0.1153	2.5034	9.9022	9.4173
0.3	8.0737	6.5274	4.8848	0.1402	2.5127	9.9022	9.4173

Table-3b : SD of fused image by PCA for different thresholds and block sizes							
th	4x4	8x8	16x16	32x32	64x64	128x128	256x256
0	49.1966	49.6046	49.9234	50.1269	50.1223	50.1231	50.1270
0.025	49.2081	49.6216	49.9234	50.1269	50.1223	50.1231	50.1270
0.05	49.2135	49.6216	49.9234	50.1269	50.1223	50.1231	50.1270
0.075	49.2137	49.6237	49.9235	50.1268	50.1223	48.3723	47.2823
0.1	49.2343	49.6237	49.9235	50.1268	50.1216	47.4560	47.2823
0.125	49.2401	49.6238	49.9235	50.1268	50.1214	47.4560	47.2823
0.15	49.2367	49.6235	49.9235	50.1268	50.1210	47.0240	47.2823
0.175	49.2784	49.6412	49.9235	50.1267	50.1210	47.0240	45.8803
0.2	49.2811	49.6412	49.9234	50.1266	50.0752	46.4345	45.8803
0.225	49.2512	49.6238	49.9234	50.1266	49.8585	45.8920	45.8803
0.25	49.2527	49.6213	49.9234	50.1267	49.8574	46.1012	45.8803
0.275	49.2497	49.6220	49.9234	50.1267	49.8576	16.1012	45.8803
0.3	49.2652	49.6218	49.7869	50.1265	49.8567	46.1012	45.8803

Table-4a : RMSE of fused image by SFA for different thresholds and block sizes							
th	4x4	8x8	16x16	32x32	64x64	128x128	256x256
0	6.9607	3.9930	2.0716	0.1861	0.2168	0.0214	0.0214
0.025	6.7950	3.7123	2.0716	0.1861	0.2168	0.0214	0.0214
0.05	6.7549	3.7123	2.0716	0.1861	0.4002	0.0214	0.0214
0.075	6.6645	3.7866	2.0716	0.1861	0.4002	0.0214	0.0214
0.1	6.6217	3.7202	2.0716	0.1861	0.4002	0.0214	0.0214
0.125	6.5846	3.5754	2.0717	0.1862	0.4002	0.0214	0.0214
0.15	6.4883	3.6633	2.0717	0.1862	0.4002	0.0214	0.0214
0.175	6.4092	3.5619	2.0570	0.1862	0.4002	0.0214	0.0214
0.2	6.3023	3.5618	2.0570	0.1862	0.4002	0.0214	0.0214
0.225	5.9935	3.5868	2.0570	0.1862	0.4002	0.0214	0.0214
0.25	5.9588	3.5869	2.0570	0.1862	0.4002	0.0214	0.0214
0.275	5.9126	3.5873	2.0570	0.1862	0.4002	0.0214	0.0214
0.3	5.8955	3.5873	2.0570	0.1862	0.4002	0.0214	0.0214

Table-4b : SD of fused image by SFA for different thresholds and block sizes

th	4x4	8x8	16x16	32x32	64x64	128x128	256x256
0	49.6070	49.9562	50.0699	50.1265	50.1262	50.1270	50.1270
0.025	49.6653	49.9744	50.0698	50.1265	50.1262	50.1270	50.1270
0.05	49.6709	49.9744	50.0698	50.1265	50.1262	50.1270	50.1270
0.075	49.7048	49.9712	50.0698	50.1265	50.1262	50.1270	50.1270
0.1	49.7127	49.9714	50.0698	50.1265	50.1262	50.1270	50.1270
0.125	49.7371	49.9786	50.0698	50.1265	50.1262	50.1270	50.1270
0.15	49.7499	49.9736	50.0699	50.1265	50.1262	50.1270	50.1270
0.175	49.7714	49.9810	50.0706	50.1265	50.1262	50.1270	50.1270
0.2	49.8036	49.9811	50.0706	50.1265	50.1262	50.1270	50.1270
0.225	49.8809	49.9792	50.0706	50.1265	50.1262	50.1270	50.1270
0.25	49.8991	49.9792	50.0706	50.1265	50.1262	50.1270	50.1270
0.275	49.8958	49.9790	50.0706	50.1265	50.1262	50.1270	50.1270
0.3	49.8886	49.9790	50.0706	50.1265	50.1262	50.1270	50.1270

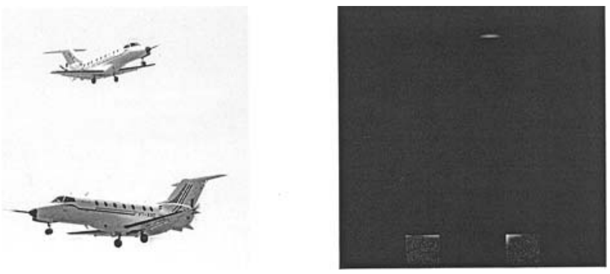

Fig.8a Fused and error images by PCA (th = 0.025 and block size 64 x 64)

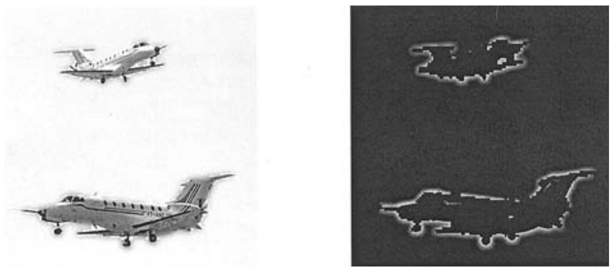

Fig.9a Fused and error images by PCA (th = 0.02 and block size 4 x 4)

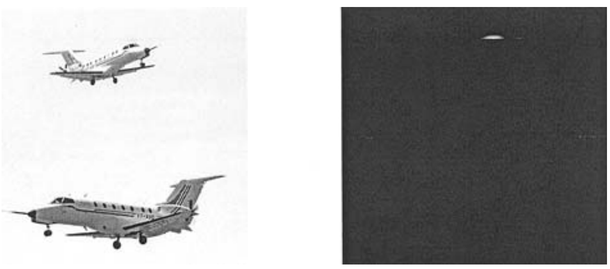

Fig.8b Fused and error images by SFA (th = 0.025 and block size 64 x 64)

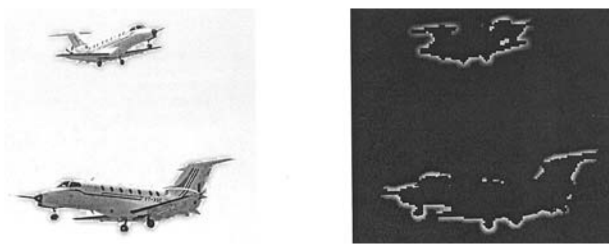

Fig.9b Fused and error images by SF (th = 0.02 and block size 4 x 4)

Table-5 : Performance evaluation metrics with block size of 64x64 and *th* = 0.025

	RMSE	PFE	PSNR	SD	SF
PCA	0.1669	0.073	55.9395	57.0859	18.8963
SF	0.161	0.0704	56.0964	57.086	18.8962

Table-6 : Performance evaluation metrics with block size of 4x4 and *th* = 0.2

	RMSE	PFE	PSNR	SD	SF
PCA	4.8068	2.102	41.3462	56.7722	18.7141
SF	4.0151	1.7558	42.1279	56.8962	18.8518

Conclusion

PCA and SF based image fusion algorithms are developed to fuse multi focused images and their performance is compared. It is concluded that SF showed slightly better performance. Block based image fusion scheme showed enhanced performance. This architecture is very simple and can be used in real time applications.

References

1. Varsheny P.K., "Multisensor Data Fusion", Elec. Comm. Engg., Journal, Vol.9 No. 12, pp. 245-253, 1997.

2. Lau Wai Leung., Bruce King and Vijay Nohora., "Comparison of Image Fusion Technique Using Entropy and INI", 22nd Asian Conference on Remote Sensing, Singapore, Nov.5-9, 2001.

3. Gonzalo Pajares and Jesus Manuel de la Cruz., "A Wavelet-based Image Fusion Tutorial", Pattern Recognition, Vol. 37, pp. 1855-1872, 2004.

4. Mallet, S.G., "A Theory for Multiresolution Signal Decomposition: The Wavelet Representation", IEEE Trans. Pattern Anal. Mach. Intel., Vol. 11, No.7, pp.674-693, 1989.

5. Wang, H., Peng, J and Wu, W., "Fusion Algorithm for Multisensor Image based on Discrete Multiwavelet Transform", IEE Pro. Vis. Image Signal Process, Vol. 149, No. 5, 2002.

6. Shutao Li., James T. Kwok and Yaonan Wang., Combination of Images with Diverse Focuses Using the Spatial Frequency", Information Fusion, Vol. 2, pp. 169-176, 2001.

7. http://en.wikipedia.org/wiki/Principal_component s_analysis.

8. Eskicioglu, A.M. and Fisher, P.S., "Image Quantity Measures and their Performance", IEEE Trans. Commun. Vol. 43, No. 12, pp.2959-2965, 1995.

9. Naidu, V.P.S., Girija, G. and Raol, J.R., "Evaluation of Data Association and Fusion Algorithms for Tracking in the Presence of Measurement Loss", AIAA Conference on Navigation, Guidance and Control, Austin, USA, August 11-14, 2003.

10. Gonzalo, R. Arce., "Nonlinear Signal Processing A Statistical Approach", Wiley-Interscience Inc., Publication, USA, 2005.

11. Rick S. Blum and Zheng Liu., "Multi-Sensor Image Fusion and its Applications", CRC Press, Taylor and Francis Group, Boca Raton, 2006.